Electronic Supplementary Material (ESI) for Dalton Transactions.

Luminescent Metal-Organic Framework based Phosphor for the Detection of Toxic Oxoanions in Aqueous Medium

Debal Kanti Singha,[a,b] Prakash Majee,[b] Sayani Hui,[a] Sudip Kumar Mondal[b]* and Partha Mahata[a]*

[a]Department of Chemistry, Jadavpur University, Kolkata-700032, India. Email: parthachem@gmail.com

[b]Department of Chemistry, Siksha-Bhavana, Visva-Bharati University, Santiniketan-731235, West Bengal, India. Email: sudip.mondal@visva-bharati.ac.in

ELECTRONIC SUPPLEMENTARY INFORMATION

Table S1: Selected bond distances (Å) observed in $[Y(FDA)(OX)_{0.5}(H_2O)_2].H_2O$, **1a**.

Bond	Distances, Å	Bond	Distances, Å
Y(1)-O(5)	2.2604(14)	Y(1)-O(3)	2.3934(14)
Y(1)-O(6)	2.2704(14)	Y(1)-O(8)	2.4003(17)
Y(1)-O(1)	2.2953(13)	Y(1)-O(4)	2.4019(13)
Y(1)-O(2)	2.3904(14)	Y(1)-O(7)	2.4117(16)

Table S2: Selected bond angles observed in $[Y(FDA)(OX)_{0.5}(H_2O)_2].H_2O$, **1a**.

Angle	Amplitude (º)	Angle	Amplitude (º)
O(5)-Y(1)-O(6)	96.75(5)	O(3)-Y(1)-O(8)	71.58(6)
O(5)-Y(1)-O(1)	143.67(5)	O(5)-Y(1)-O(4)	74.39(5)
O(6)-Y(1)-O(1)	100.62(5)	O(6)-Y(1)-O(4)	77.72(5)
O(5)-Y(1)-O(2)	142.35(5)	O(1)-Y(1)-O(4)	140.49(5)
O(6)-Y(1)-O(2)	71.51(5)	O(2)-Y(1)-O(4)	68.22(5)
O(1)-Y(1)-O(2)	73.84(5)	O(3)-Y(1)-O(4)	76.46(5)
O(5)-Y(1)-O(3)	100.12(5)	O(8)-Y(1)-O(4)	128.18(6)
O(6)-Y(1)-O(3)	143.88(6)	O(5)-Y(1)-O(7)	76.82(6)
O(1)-Y(1)-O(3)	84.06(5)	O(6)-Y(1)-O(7)	73.26(6)
O(2)-Y(1)-O(3)	75.66(5)	O(1)-Y(1)-O(7)	78.03(6)
O(5)-Y(1)-O(8)	72.45(6)	O(2)-Y(1)-O(7)	129.17(6)
O(6)-Y(1)-O(8)	144.39(7)	O(3)-Y(1)-O(7)	141.78(6)
O(1)-Y(1)-O(8)	74.88(6)	O(8)-Y(1)-O(7)	71.25(7)
O(2)-Y(1)-O(8)	136.40(6)	O(4)-Y(1)-O(7)	135.88(6)

Table S3: Average lifetime of the ligand center (at 375 nm) of compound **1** after the addition of different analytes.

Sl. No	**K_2CrO_4**	a_1	a_2	τ_1	τ_2	$a_1\tau_1 + a_2\tau_2$
1	0 μM	0.74	0.26	1.2	6.1	2.5 ns
2	0.312 μM	0.72	0.28	1.2	5.8	2.5 ns
3	1.25 μM	0.71	0.29	1.2	5.8	2.5 ns
4	5.00 μM	0.72	0.28	1.2	5.9	2.5 ns
5	10.0 μM	0.71	0.29	1.1	5.7	2.4 ns
Sl. No	**$KMnO_4$**	a_1	a_2	τ_1	τ_2	$a_1\tau_1 + a_2\tau_2$
1	0 μM	0.72	0.28	1.2	5.8	2.5 ns
2	0.312 μM	0.74	0.26	1.3	6.4	2.6 ns
3	1.25 μM	0.73	0.27	1.2	6.2	2.6 ns
4	5.00 μM	0.74	0.26	1.2	6.3	2.5 ns
5	10.0 μM	0.72	0.28	1.2	6.0	2.5 ns
Sl. No	**Na_2HPO_4**	a_1	a_2	τ_1	τ_2	$a_1\tau_1 + a_2\tau_2$
1	0 μM	0.75	0.25	1.3	6.4	2.6 ns
2	1.25 μM	0.73	0.27	1.2	6.2	2.5 ns
3	2.50 μM	0.74	0.26	1.3	6.4	2.6 ns
4	5.00 μM	0.73	0.27	1.2	6.0	2.5 ns
5	7.50 μM	0.74	0.26	1.2	6.3	2.5 ns
6	10.0 μM	0.72	0.28	1.1	5.8	2.4 ns

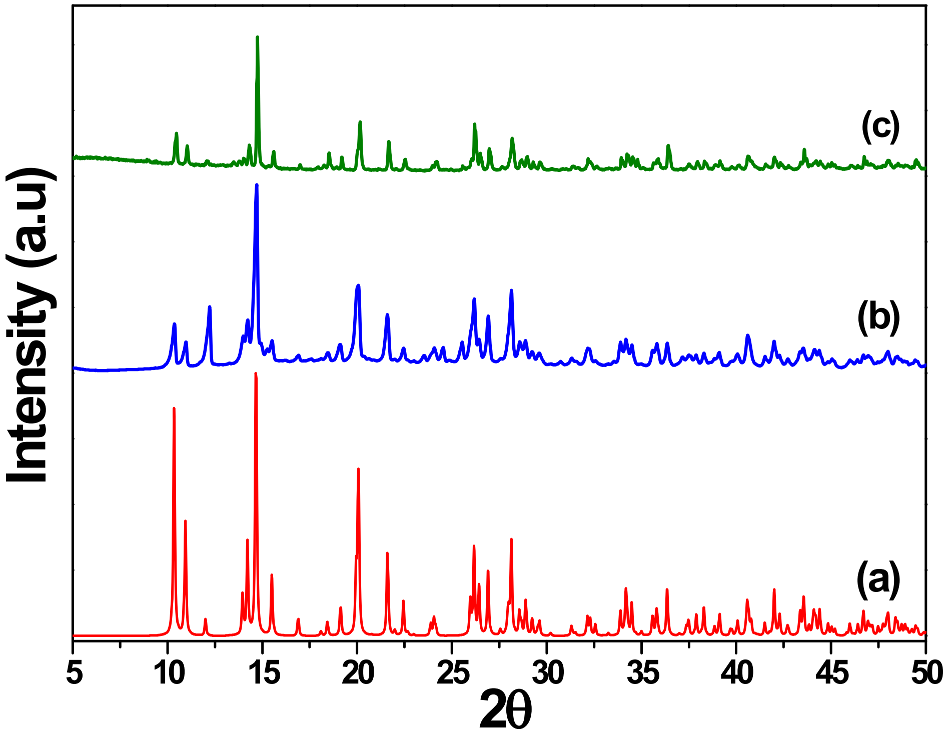

Fig. S1: Powder XRD (CuKα) patterns: (a) simulated from single crystal X-ray data of $[Y(FDA)(Ox)_{0.5}(H_2O)_2]\cdot H_2O$, **1a**, (b) hydrothermally synthesized $[Y(FDA)(Ox)_{0.5}(H_2O)_2]\cdot H_2O$, **1a** and (c) hydrothermally synthesized $[Tb_{0.2}Y_{0.8}(FDA)(Ox)_{0.5}(H_2O)_2]\cdot H_2O$, **1**.

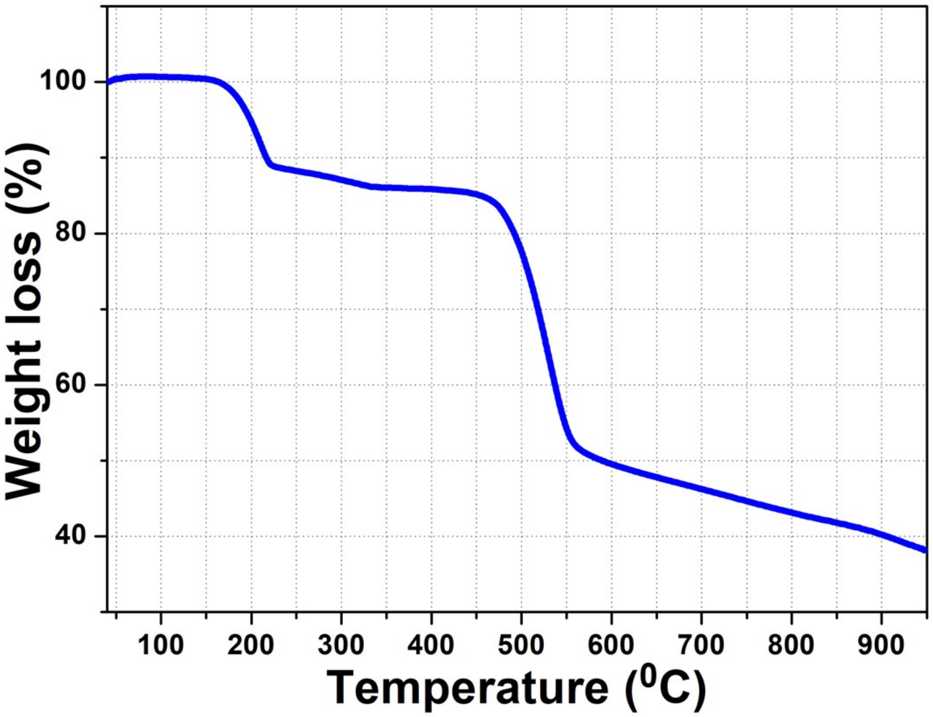

Fig. S2: Thermogravimetric analysis (TGA) of compound **1** in nitrogen atmosphere.

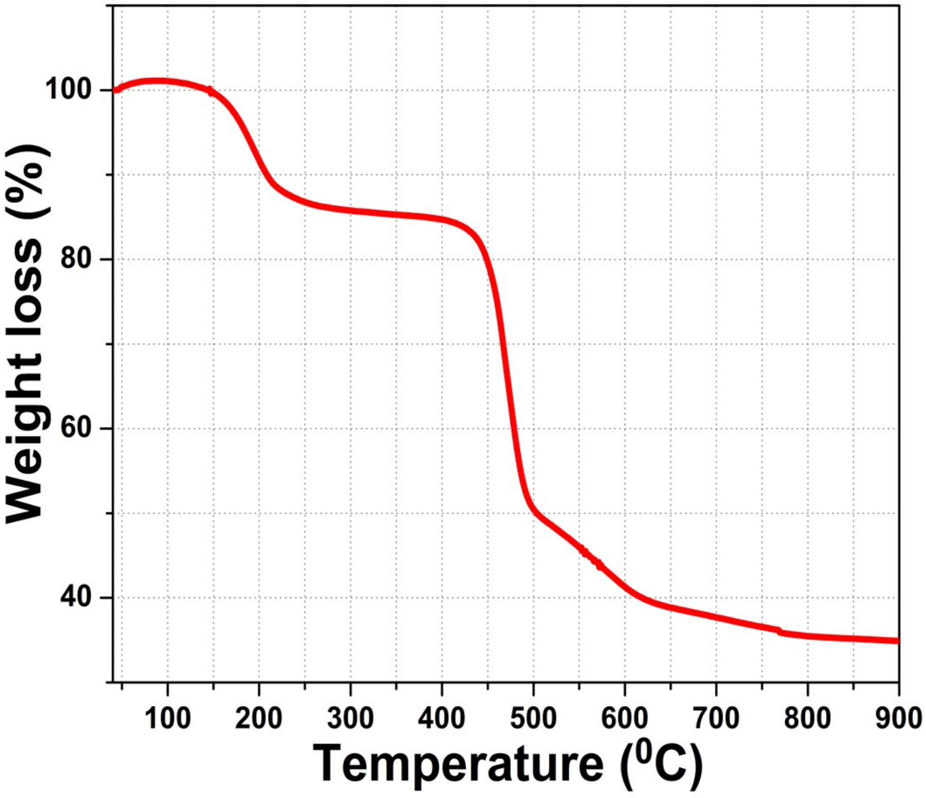

Fig. S3: Thermogravimetric analysis (TGA) of compound **1a** in nitrogen atmosphere.

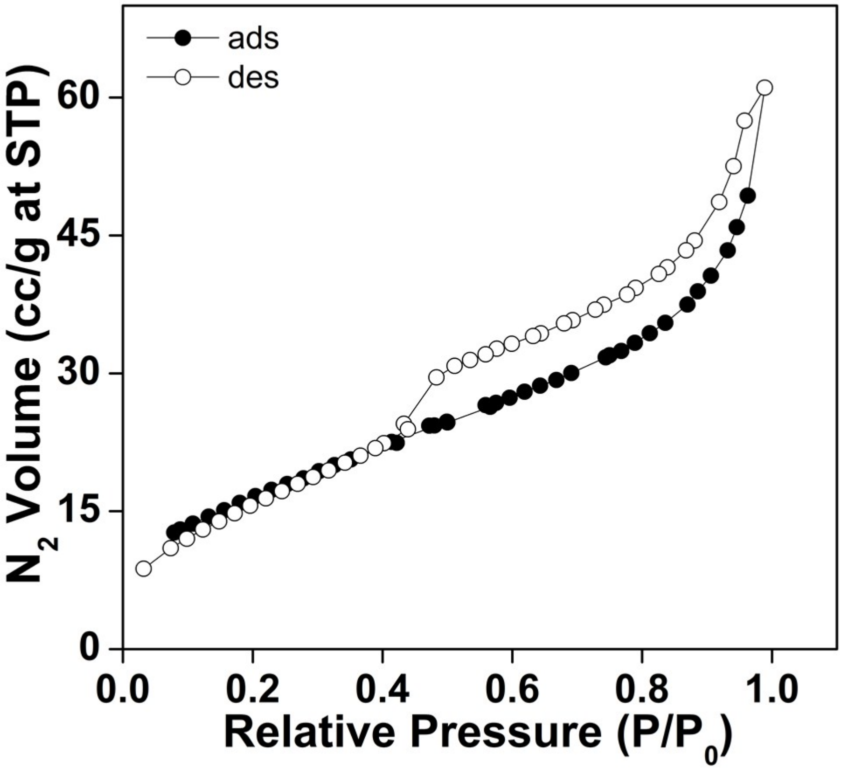

Fig. S4: N_2 sorption isotherm of compound **1**.

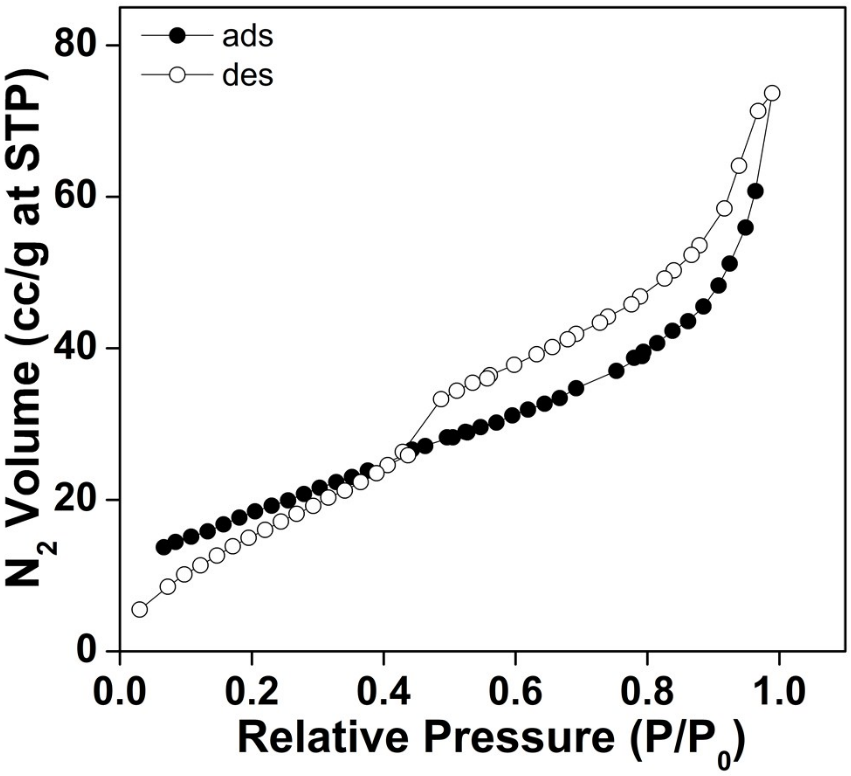

Fig. S5: N_2 sorption isotherm of compound **1a**.

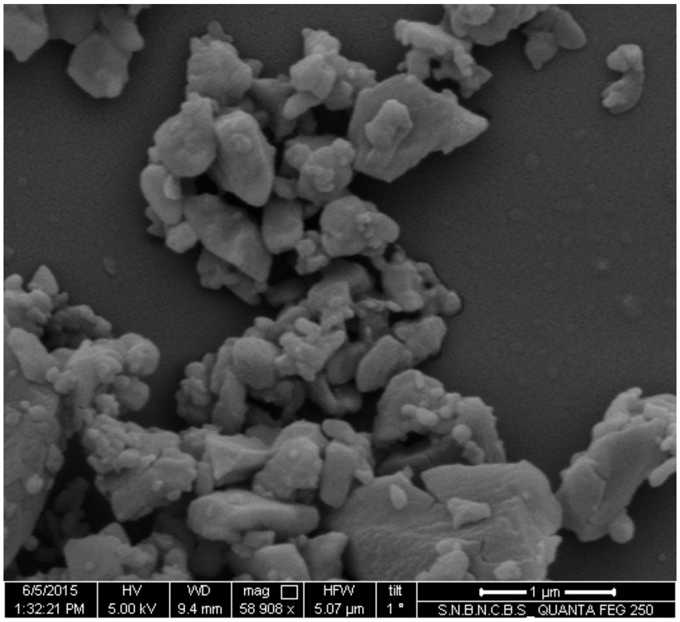

Fig. S6: SEM images of compound **1**.

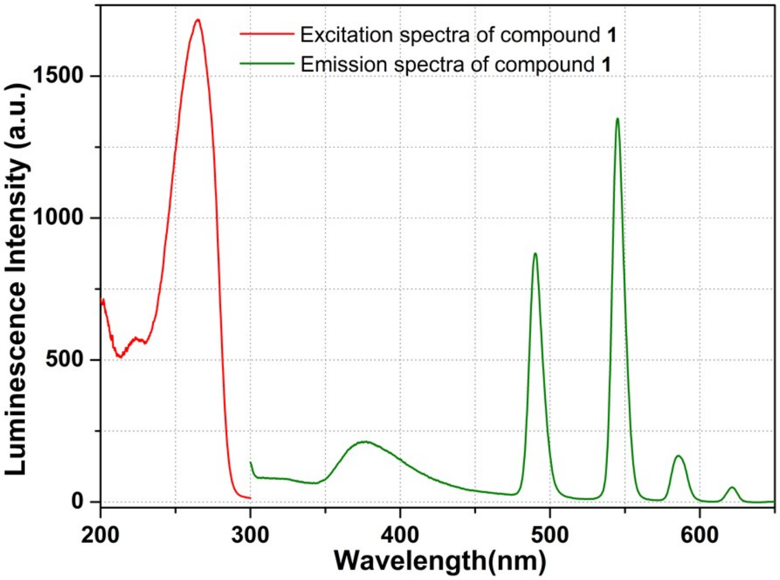

Fig. S7: Excitation spectra (monitored at λ_{em} = 545 nm), ligand center emission spectra and Tb center luminescence spectra (excited at 265 nm) of compound **1**.

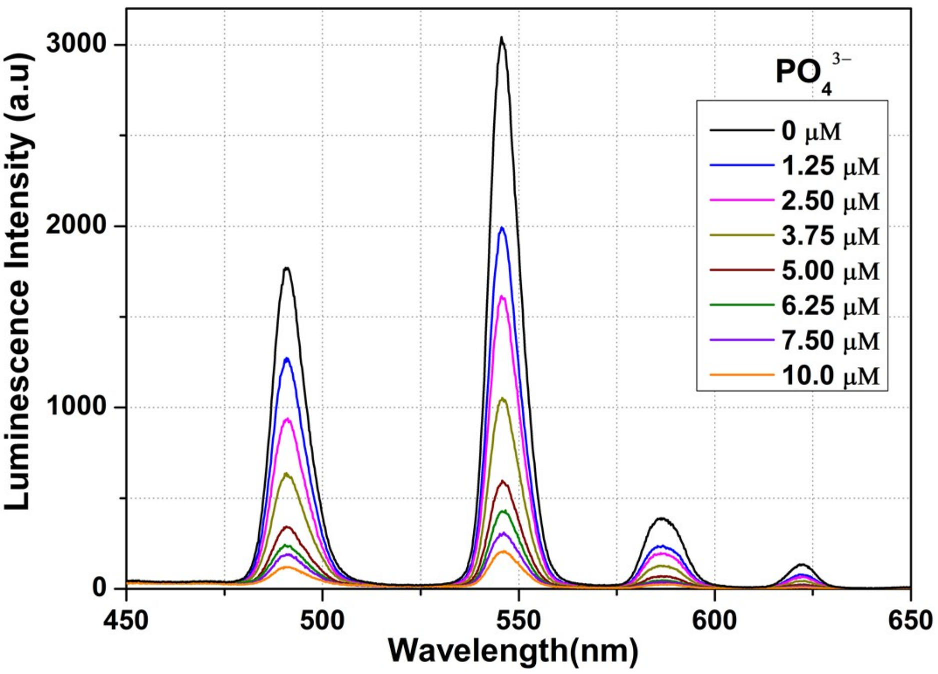

Fig. S8: Emission spectra of compound **1** in aqueous dispersion upon incremental addition of aqueous solution of PO_4^{3-} ions (λ_{ex} = 265 nm). Final concentration of PO_4^{3-} ions in the medium is indicated in the legend.

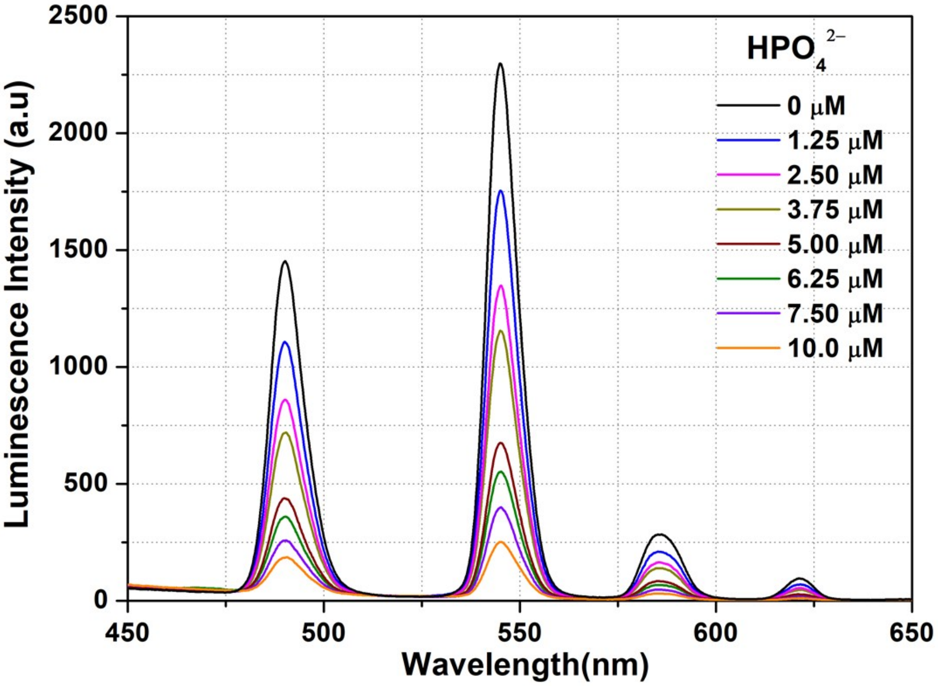

Fig. S9: Emission spectra of compound **1** in aqueous dispersion upon incremental addition of aqueous solution of HPO_4^{2-} ions (λ_{ex} = 265 nm). Final concentration of HPO_4^{2-} ions in the medium is indicated in the legend.

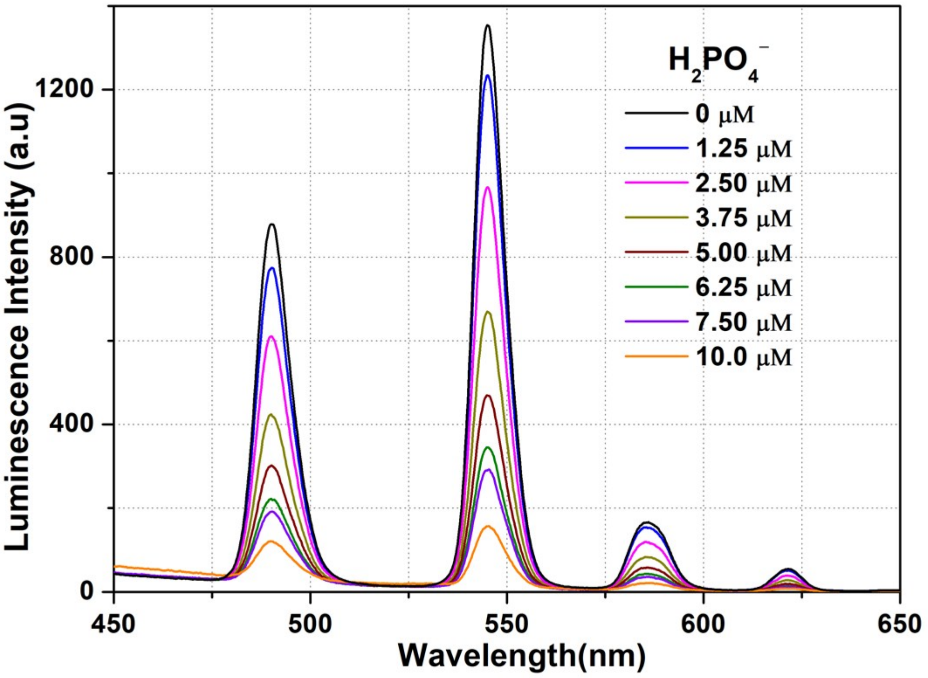

Fig. S10: Emission spectra of compound **1** in aqueous dispersion upon incremental addition of aqueous solution of $H_2PO_4^-$ ions (λ_{ex} = 265 nm). Final concentration of $H_2PO_4^-$ ions in the medium is indicated in the legend.

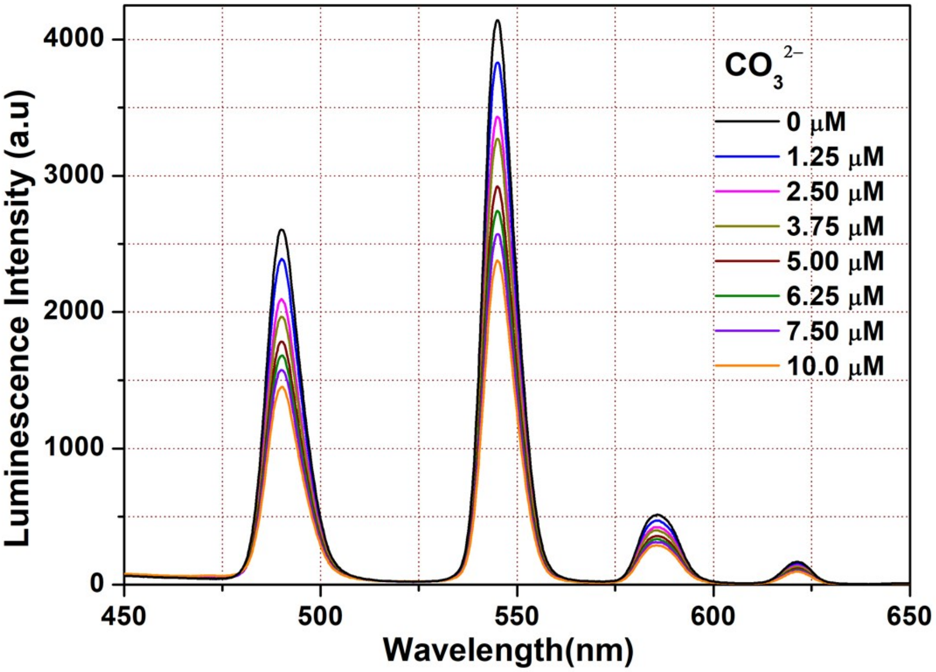

Fig. S11: Emission spectra of compound **1** in aqueous dispersion upon incremental addition of aqueous solution of CO_3^{2-} ions (λ_{ex} = 265 nm). Final concentration of CO_3^{2-} ions in the medium is indicated in the legend.

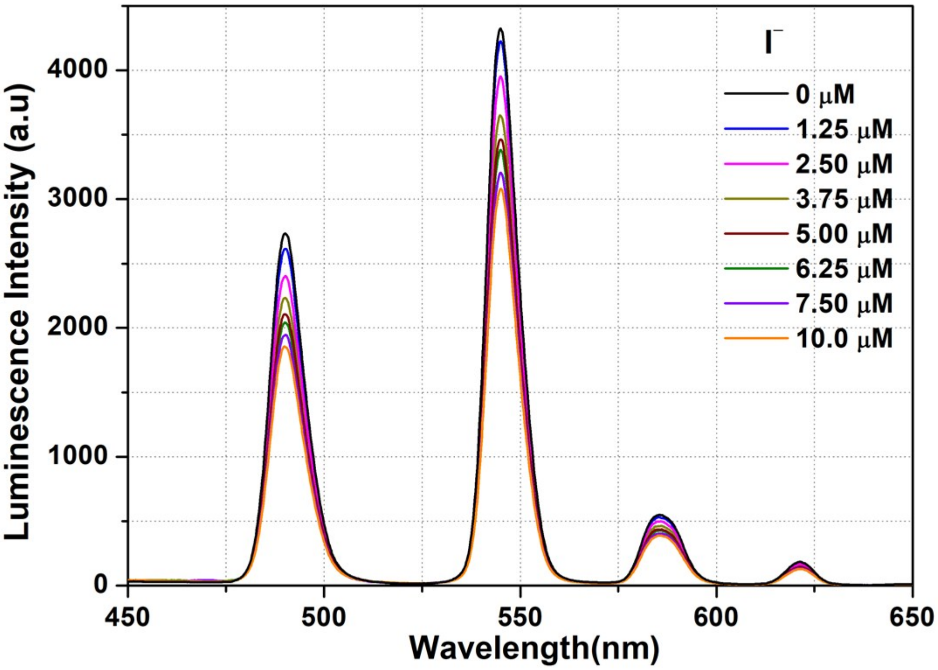

Fig. S12: Emission spectra of compound **1** in aqueous dispersion upon incremental addition of aqueous solution of I^- ions (λ_{ex} = 265 nm). Final concentration of I^- ions in the medium is indicated in the legend.

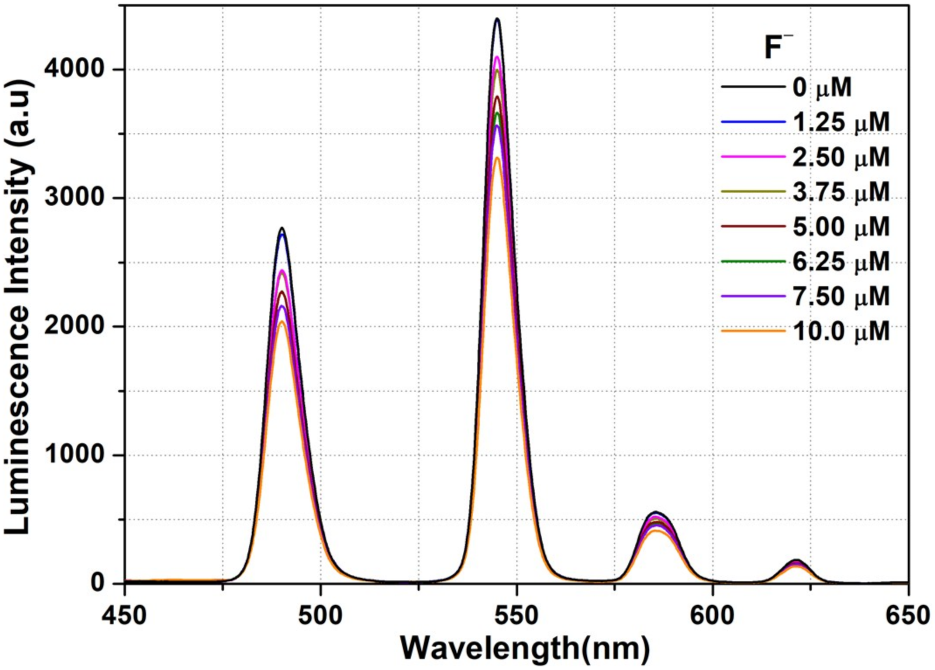

Fig. S13: Emission spectra of compound **1** in aqueous dispersion upon incremental addition of aqueous solution of F^- ions (λ_{ex} = 265 nm). Final concentration of F^- ions in the medium is indicated in the legend.

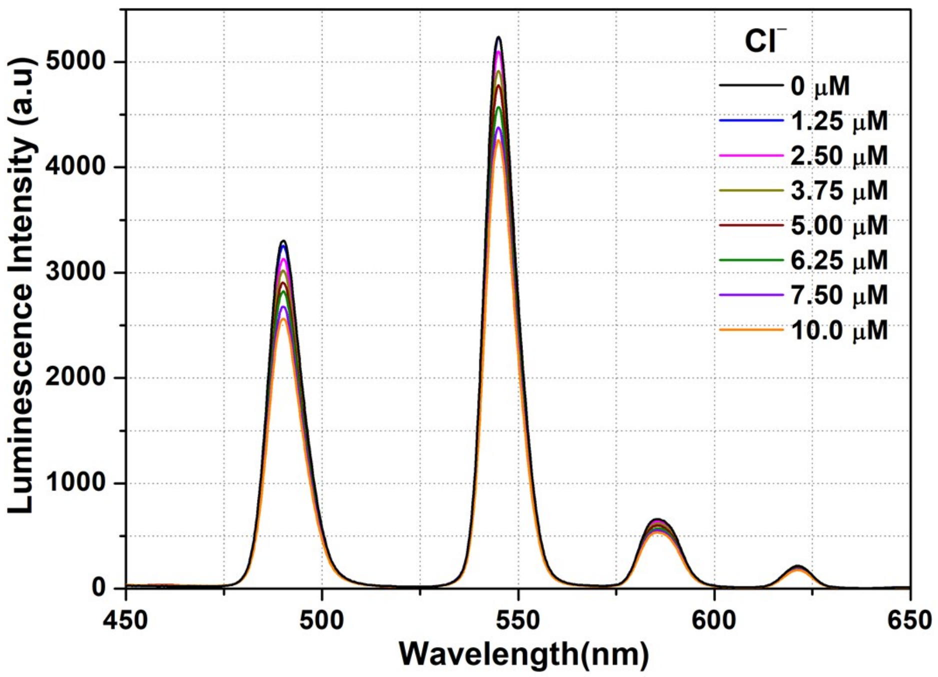

Fig. S14: Emission spectra of compound **1** in aqueous dispersion upon incremental addition of aqueous solution of Cl^- ions (λ_{ex} = 265 nm). Final concentration of Cl^- ions in the medium is indicated in the legend.

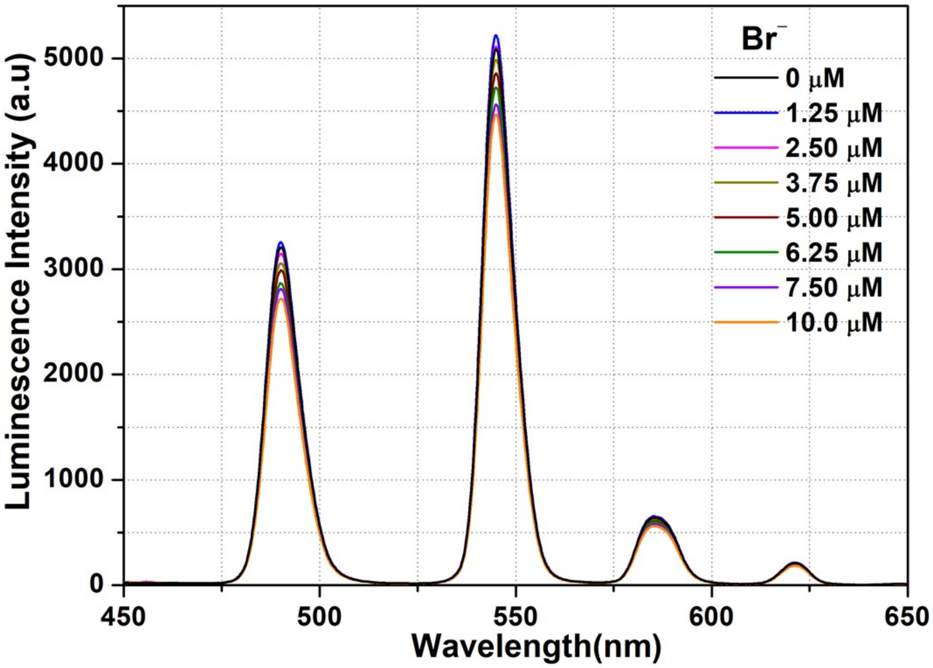

Fig. S15: Emission spectra of compound **1** in aqueous dispersion upon incremental addition of aqueous solution of Br^- ions (λ_{ex} = 265 nm). Final concentration of Br^- ions in the medium is indicated in the legend.

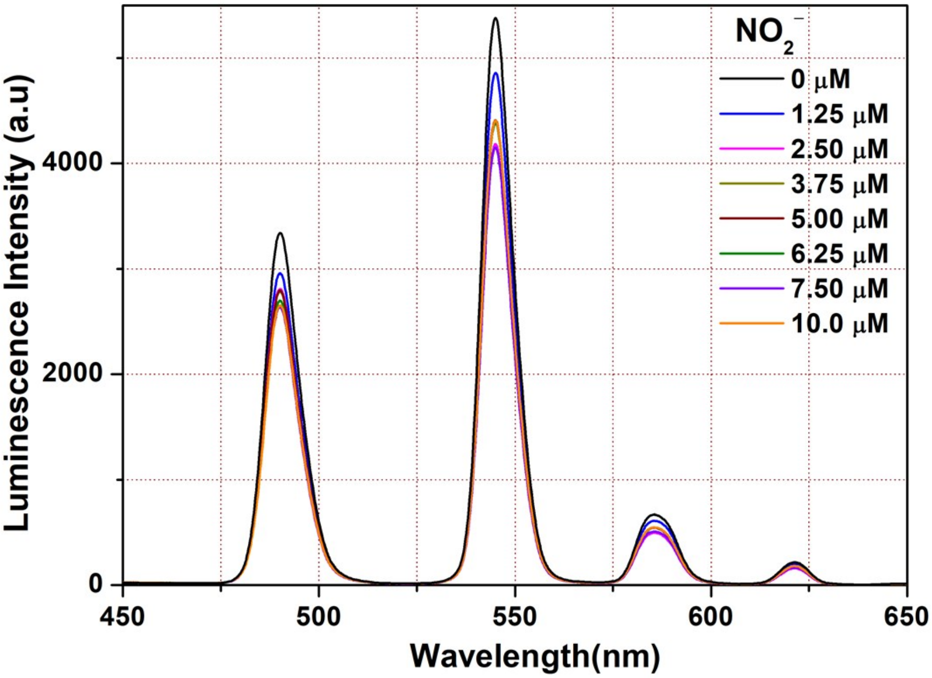

Fig. S16: Emission spectra of compound **1** in aqueous dispersion upon incremental addition of aqueous solution of NO_2^- ions (λ_{ex} = 265 nm). Final concentration of NO_2^- ions in the medium is indicated in the legend.

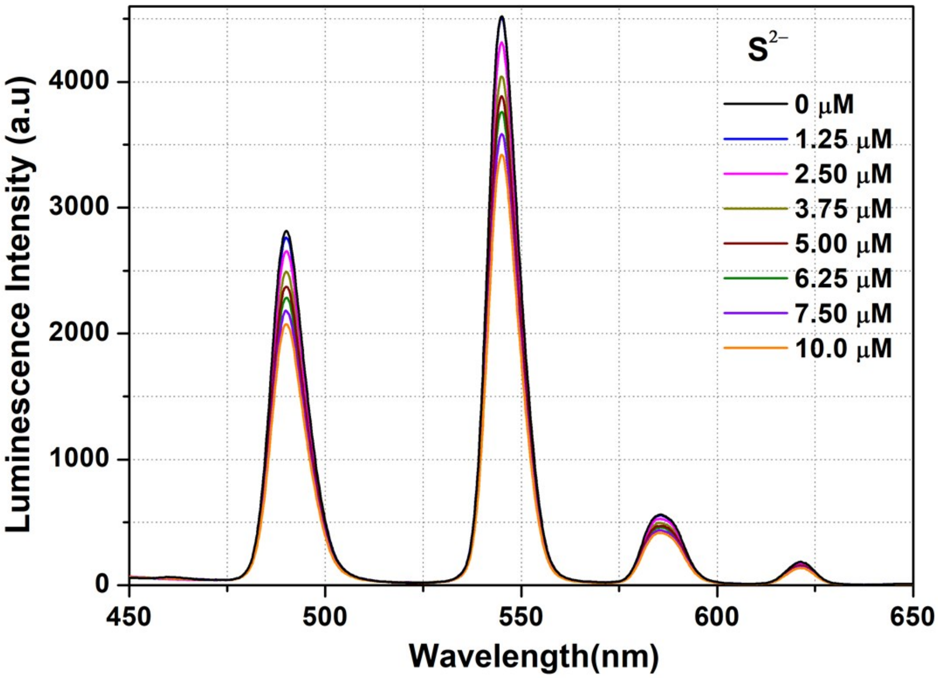

Fig. S17: Emission spectra of compound **1** in aqueous dispersion upon incremental addition of aqueous solution of S^{2-} ions (λ_{ex} = 265 nm). Final concentration of S^{2-} ions in the medium is indicated in the legend.

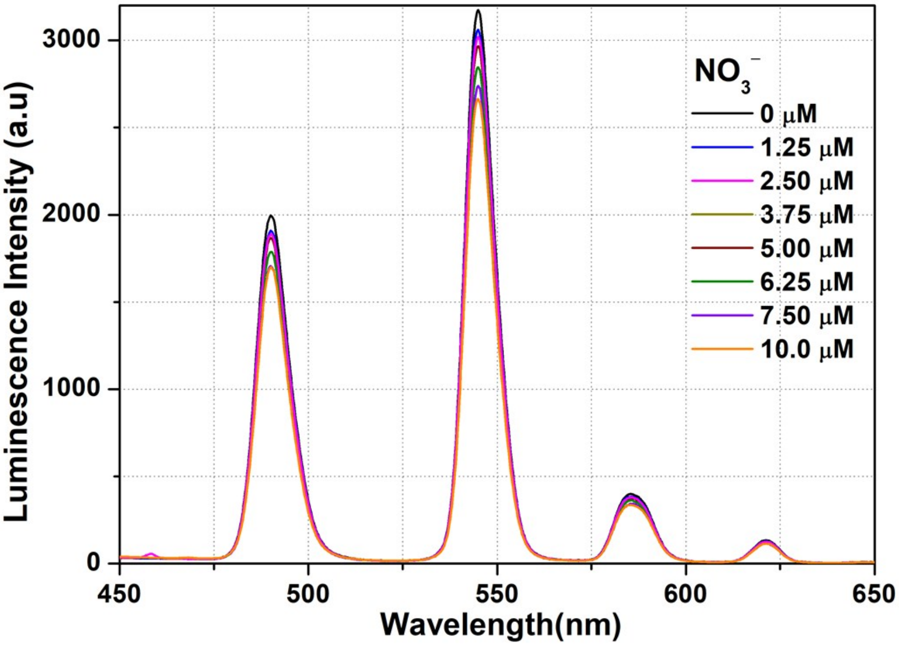

Fig. S18: Emission spectra of compound **1** in aqueous dispersion upon incremental addition of aqueous solution of NO_3^- ions (λ_{ex} = 265 nm). Final concentration of NO_3^- ions in the medium is indicated in the legend.

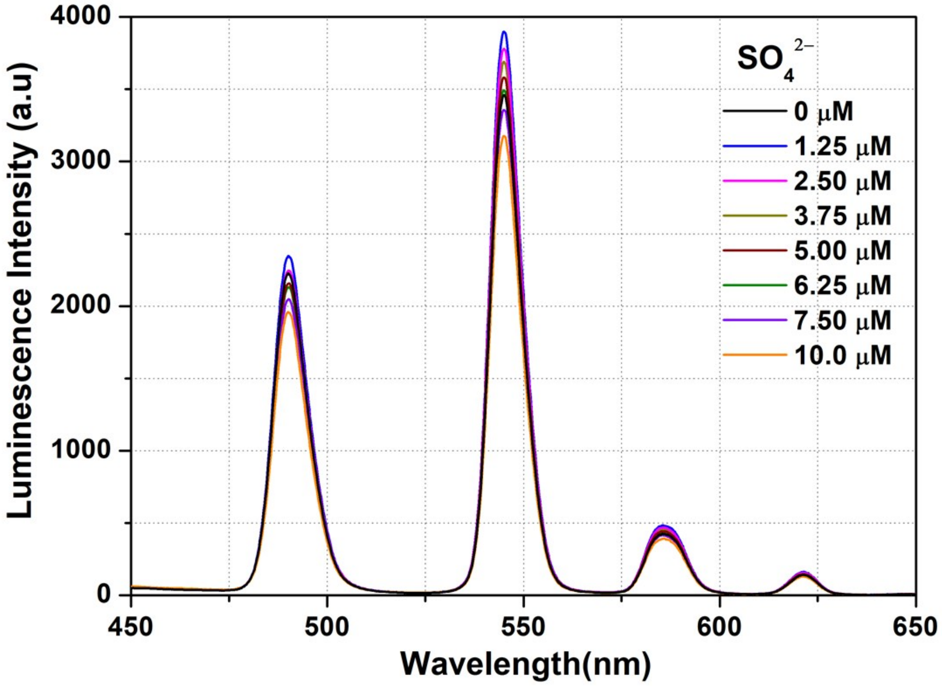

Fig. S19: Emission spectra of compound **1** in aqueous dispersion upon incremental addition of aqueous solution of SO_4^{2-} ions (λ_{ex} = 265 nm). Final concentration of SO_4^{2-} ions in the medium is indicated in the legend.

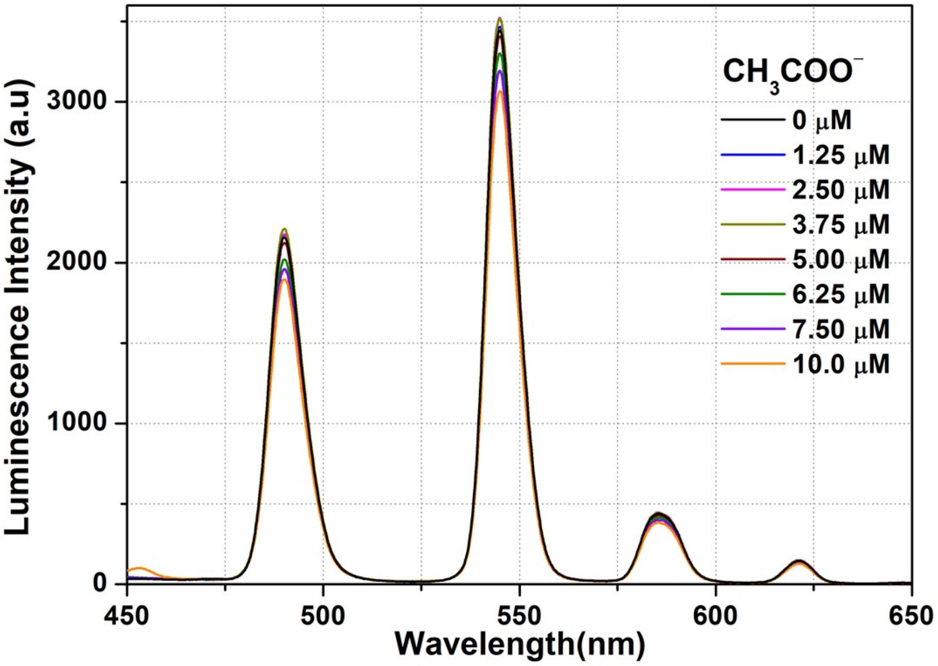

Fig. S20: Emission spectra of compound **1** in aqueous dispersion upon incremental addition of aqueous solution of CH_3COO^- ions (λ_{ex} = 265 nm). Final concentration of CH_3COO^- ions in the medium is indicated in the legend.

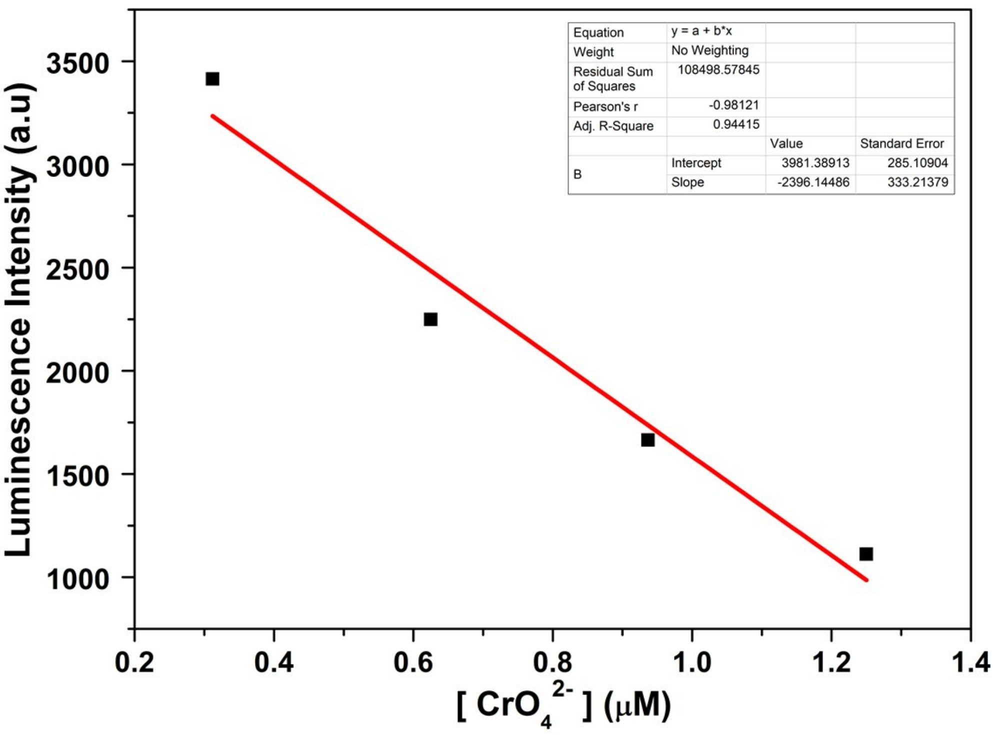

Equation	y = a + b*x		
Weight	No Weighting		
Residual Sum of Squares	108498.57845		
Pearson's r	-0.98121		
Adj. R-Square	0.94415		
		Value	Standard Error
B	Intercept	3981.38913	285.10904
	Slope	-2396.14486	333.21379

Fig. S21: Plot of luminescence intensity *vs* concentration of CrO_4^{2-}.

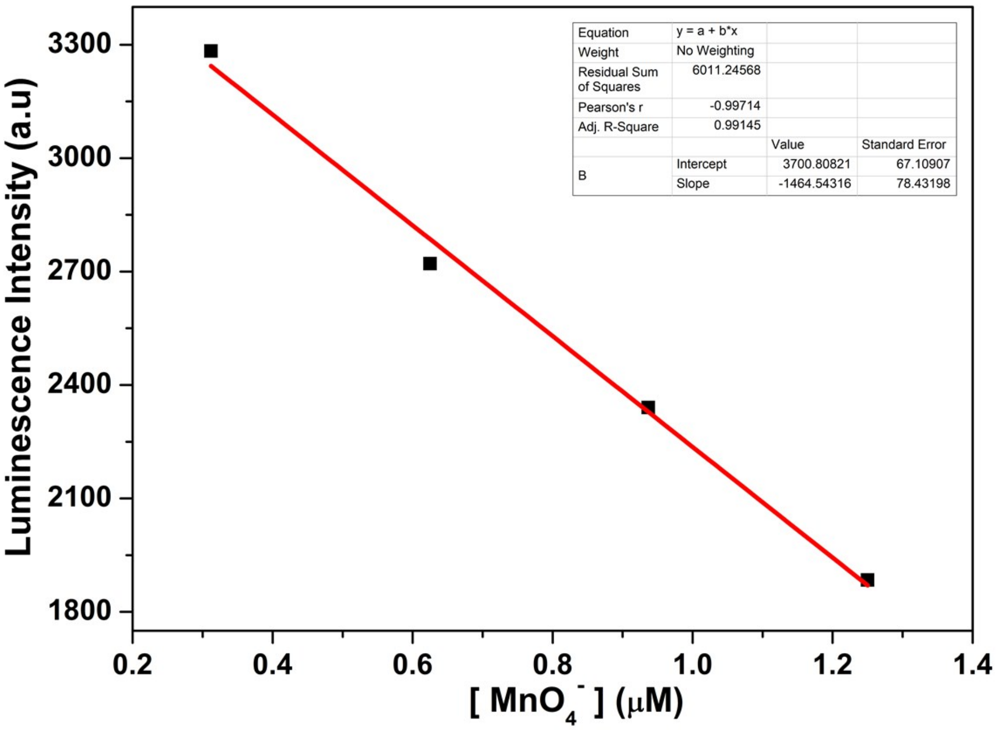

Equation	y = a + b*x		
Weight	No Weighting		
Residual Sum of Squares	6011.24568		
Pearson's r	-0.99714		
Adj. R-Square	0.99145		
		Value	Standard Error
B	Intercept	3700.80821	67.10907
	Slope	-1464.54316	78.43198

Fig. S22: Plot of luminescence intensity *vs* concentration of MnO_4^-.

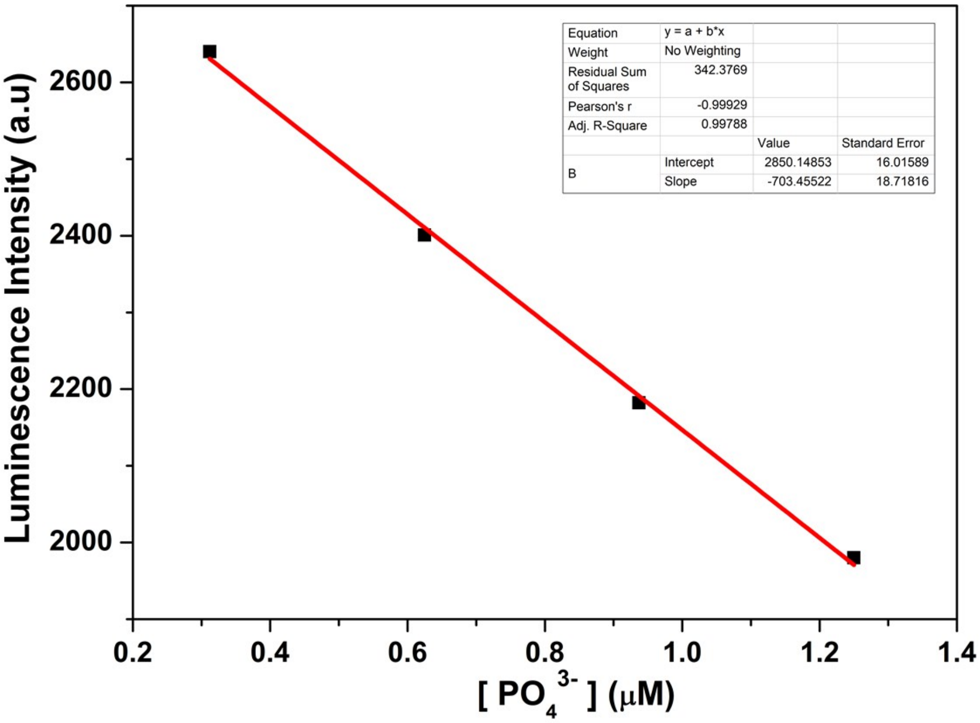

Equation	y = a + b*x		
Weight	No Weighting		
Residual Sum of Squares	342.3769		
Pearson's r	-0.99929		
Adj. R-Square	0.99788		
		Value	Standard Error
B	Intercept	2850.14853	16.01589
	Slope	-703.45522	18.71816

Fig. S23: Plot of luminescence intensity *vs* concentration of phosphate.

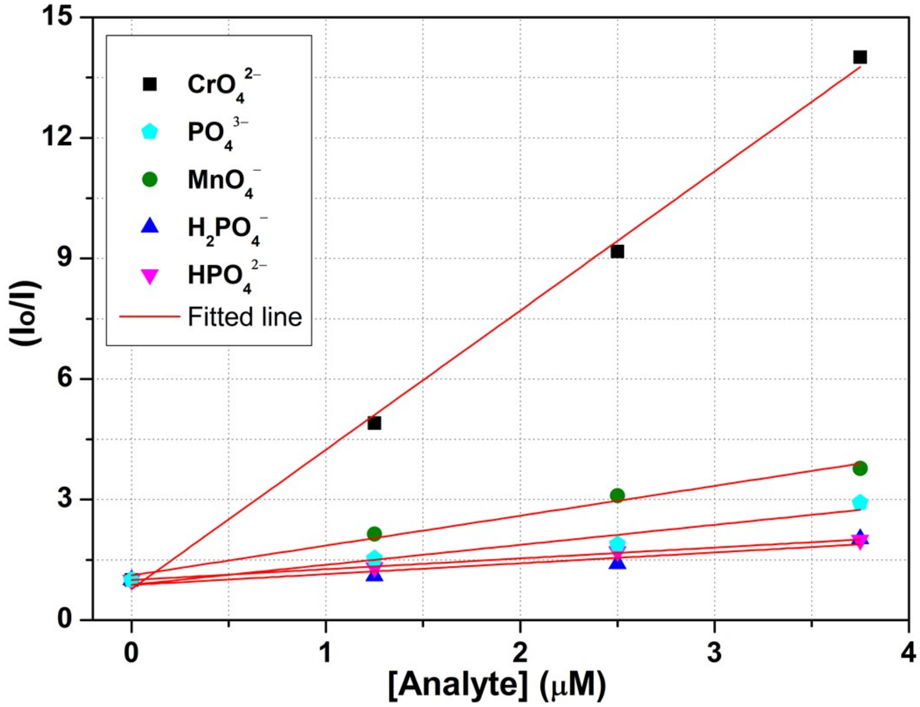

Fig. S24: Plot of I_0/I of compound **1** (at 545 nm) vs concentration of analytes in the lower concentration range of analytes (up to 3.75 μM). I_0 and I are the luminescence intensity in absence and presence of analyte, respectively.

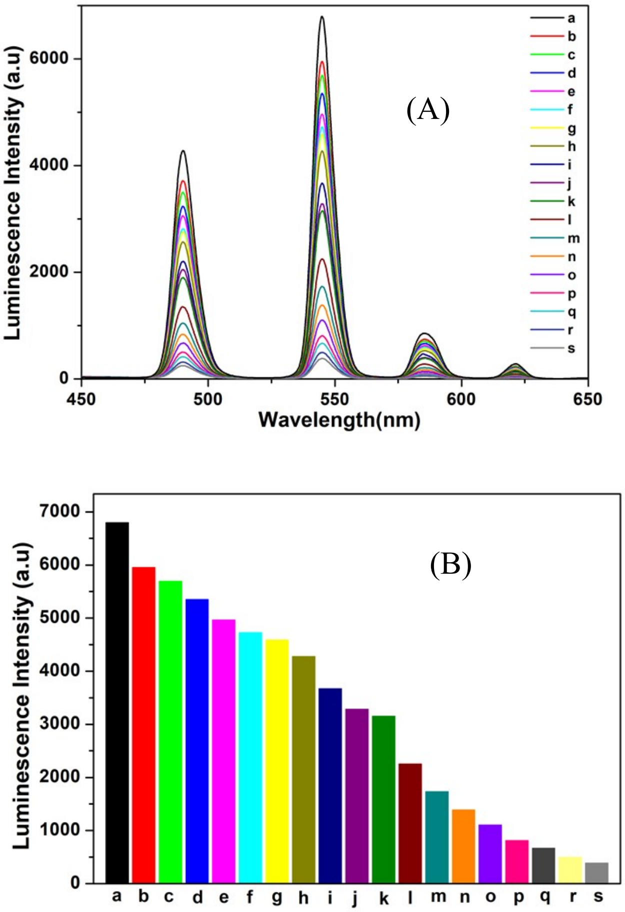

Fig. S25: (A) Emission spectra of compound **1** in aqueous solution upon the incremental addition of MnO_4^- solution in presence of 12.5 μM of each quenchable metal ions solution (λ_{ex} = 265 nm). (B) Corresponding bar diagram showing the luminescence intensity (monitored at 545 nm) after the sequential addition of the analytes. The composition and concentration of the system were as follows: (a) compound **1** in aqueous dispersion, (b) a + 12.5 μM F^-, (c) b + 12.5 μM Cl^-, (d) c + 12.5 μM Br^-, (e) d + 12.5 μM I^-, (f) e + 12.5 μM NO_3^-, (g) f + 12.5 μM NO_2^-, (h) g + 12.5 μM SO_4^{2-}, (i) h + 12.5 μM CO_3^{2-}, (j) i + 12.5 μM CH_3COO^-, (k) j + 12.5 μM S^{2-}, (l) k + 1.25 μM MnO_4^-, (m) k + 2.50 μM MnO_4^-, (n) k + 3.75 μM MnO_4^-, (o) k + 5.00 μM MnO_4^-, (p) k + 6.25 μM MnO_4^-, (r) k + 7.50 μM MnO_4^- and (s) k + 10.00 μM MnO_4^-.

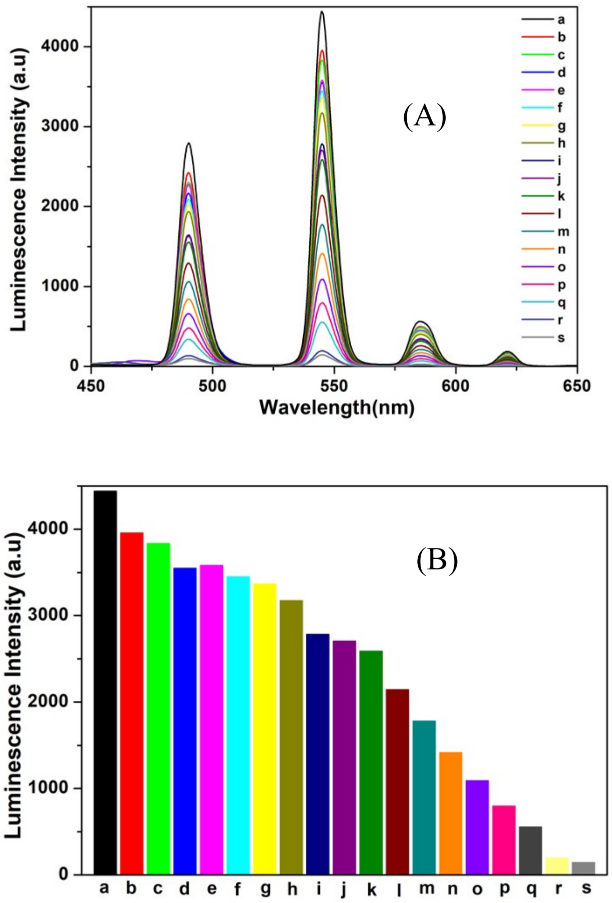

Fig. S26: (A) Emission spectra of compound **1** in aqueous solution upon the incremental addition of HPO_4^{2-} solution in presence of 12.5 µM of each quenchable metal ions solution (λ_{ex} = 265 nm). (B) Corresponding bar diagram showing the luminescence intensity (monitored at 545 nm) after the sequential addition of the analytes. The composition and concentration of the system were as follows: (a) compound **1** in aqueous dispersion, (b) a + 12.5 µM F^-, (c) b + 12.5 µM Cl^-, (d) c + 12.5 µM Br^-, (e) d + 12.5 µM I^-, (f) e + 12.5 µM NO_3^-, (g) f + 12.5 µM NO_2^-, (h) g + 12.5 µM SO_4^{2-}, (i) h + 12.5 µM CO_3^{2-}, (j) i + 12.5 µM CH_3COO^-, (k) j + 12.5 µM S^{2-}, (l) k + 1.25 µM HPO_4^{2-}, (m) k + 2.50 µM HPO_4^{2-}, (n) k + 3.75 µM HPO_4^{2-}, (o) k + 5.00 µM HPO_4^{2-}, (p) k + 6.25 µM HPO_4^{2-}, (r) k + 7.50 µM HPO_4^{2-} and (s) k + 10.00 µM HPO_4^{2-}.

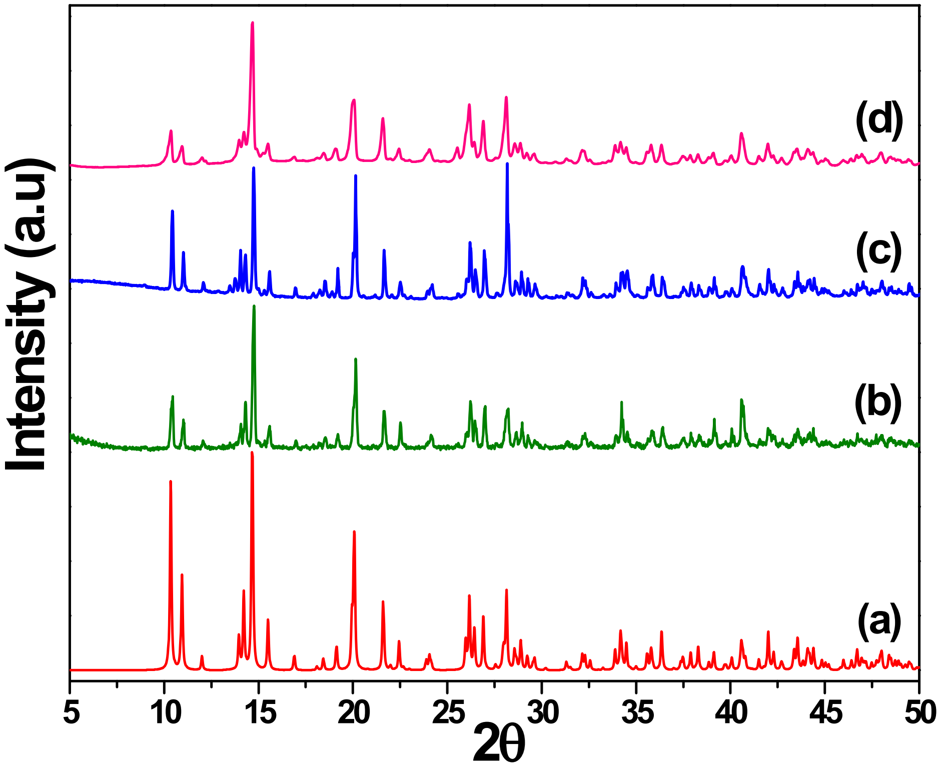

Fig. S27: Powder XRD (CuKα) patterns of (a) compound **1a** simulated from single crystal X-ray data, (b) compound **1** after immersing in the aqueous solution of CrO_4^{2-} for 24 hours, (c) compound **1** after immersing in the aqueous solution of MnO_4^- for 24 hours and (d) compound **1** after immersing in the aqueous solution of HPO_4^{2-} for 24 hours.

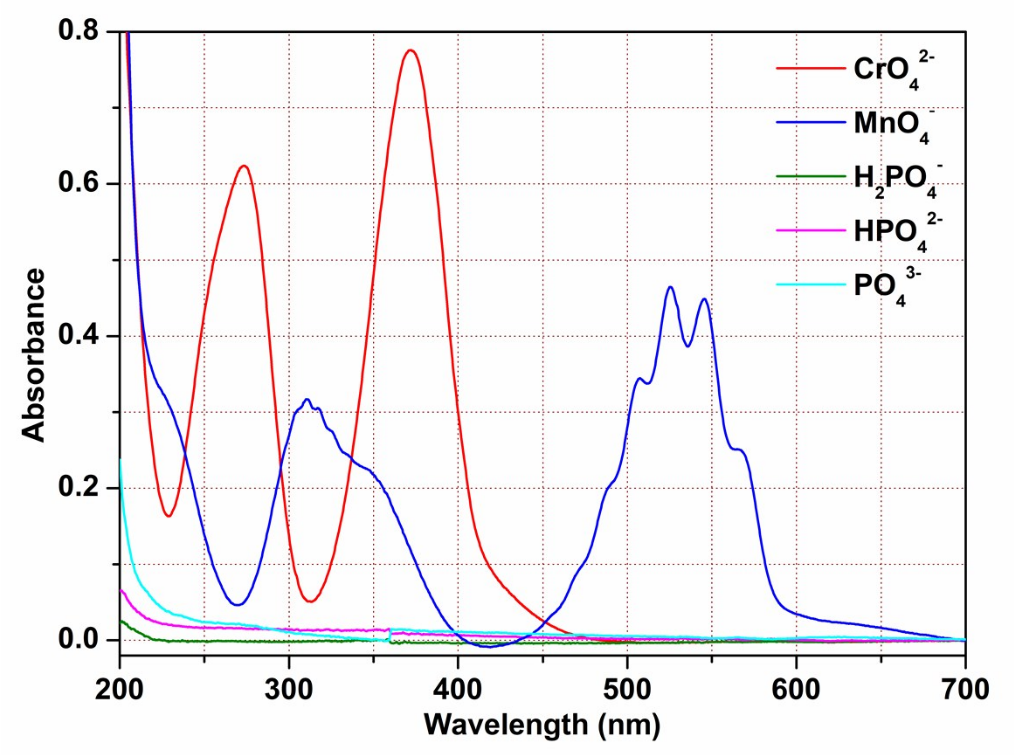

Fig. S28: Absorption spectra of different anions at the same concentration (~ 200 μM).

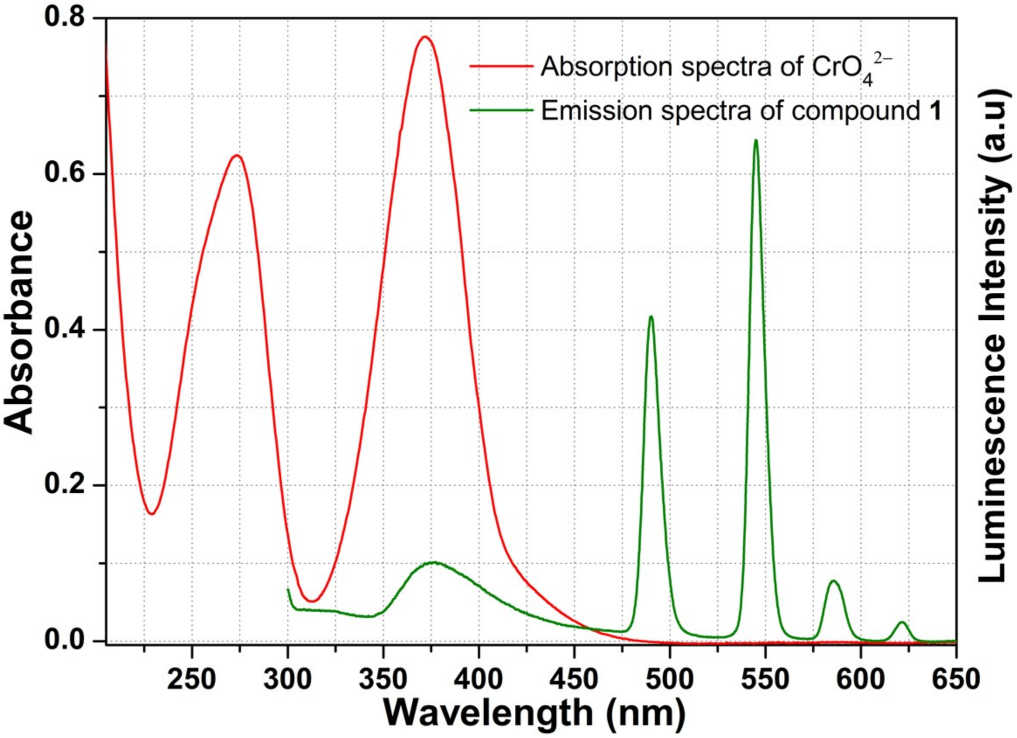

Fig. S29: Absorption spectra of CrO_4^{2-} and emission spectra of compound **1**.

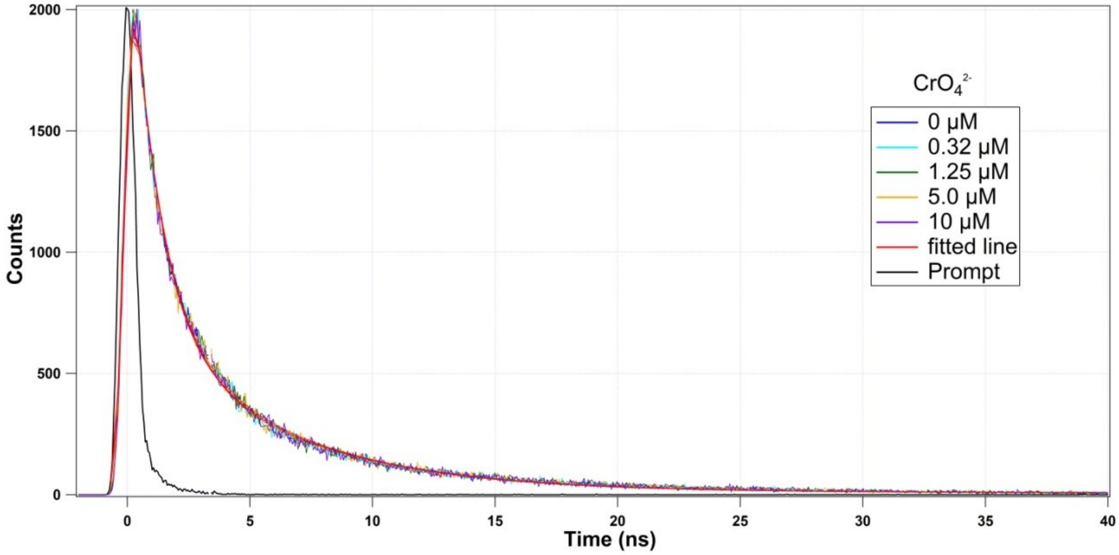

Figure S30: Time resolved luminescence decay and the corresponding fitted lines of compound **1** with the gradual addition of CrO_4^{2-} ions. Final concentrations of metal ions in the medium are indicated in the legend. The instrument response function (prompt) is also shown. The λ_{ex} = 280 nm and λ_{em} = 375 nm were used in this experiment.

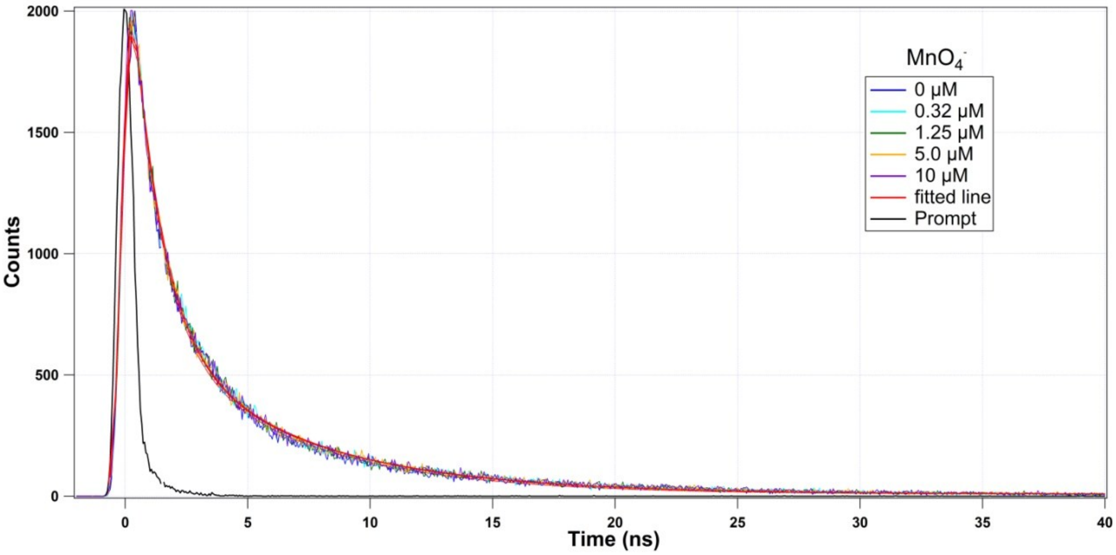

Figure S31: Time resolved luminescence decay and the corresponding fitted lines of compound **1** with the gradual addition of MnO$_4^-$ ions. Final concentrations of metal ions in the medium are indicated in the legend. The instrument response function (prompt) is also shown. The λ_{ex} = 280 nm and λ_{em} = 375 nm were used in this experiment.

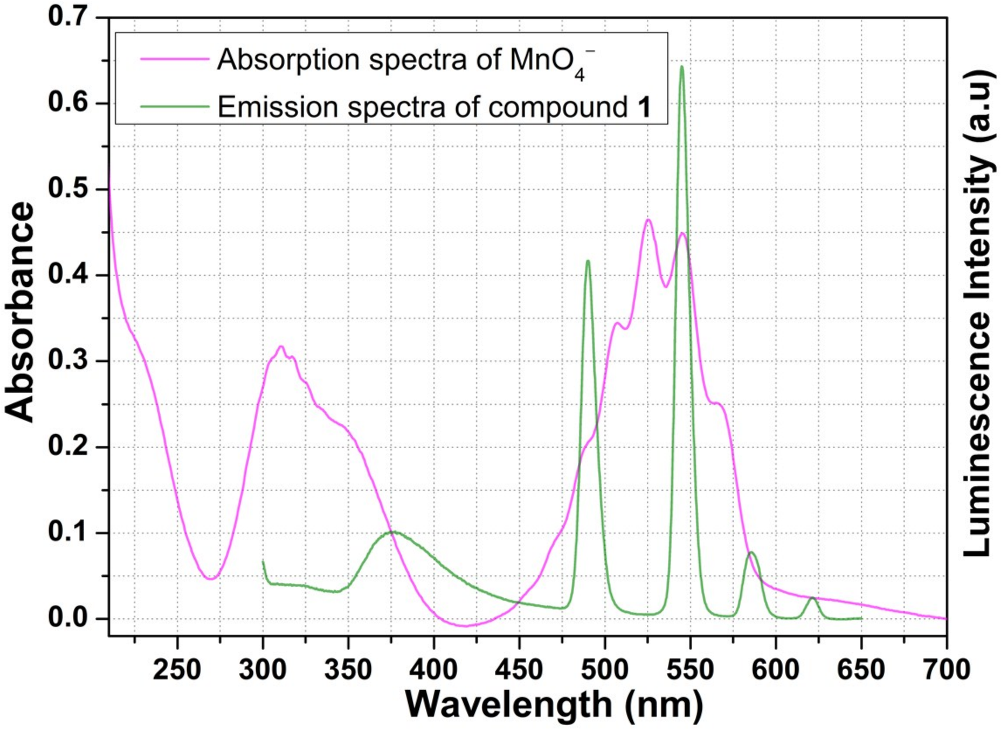

Fig. S32: Absorption spectra of MnO_4^- and emission spectra of compound **1**.

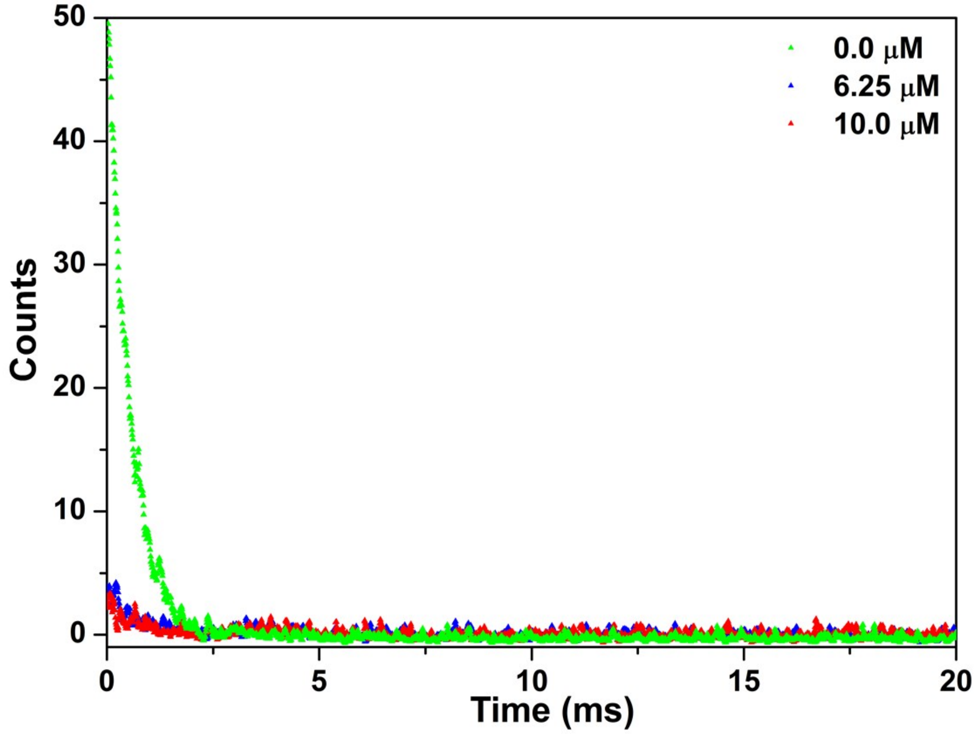

Fig. S33: The luminescence lifetime decay curve of compound **1** and in presence of MnO_4^- ions in aqueous medium at 545 nm. The Tb centre lifetime values are 524 μs, 327 μs and 206 μs after the addition of 0 μM, 6.25 μM and 10 μM MnO_4^- respectively.

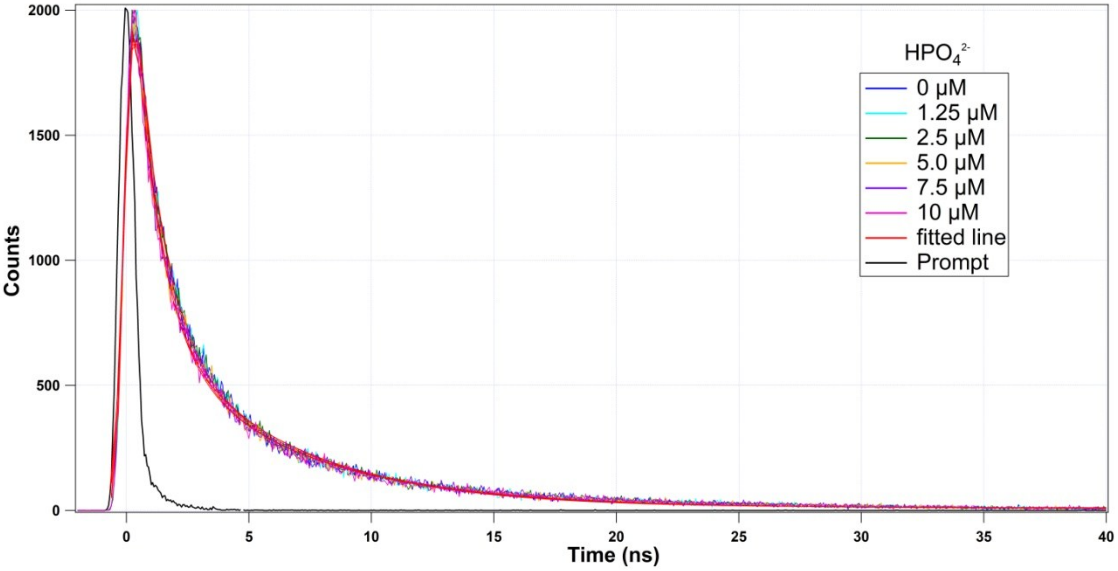

Figure S34: Time resolved luminescence decay and the corresponding fitted lines of compound **1** with the gradual addition of HPO_4^{2-} ions. Final concentrations of metal ions in the medium are indicated in the legend. The instrument response function (prompt) is also shown. The λ_{ex} = 280 nm and λ_{em} = 375 nm were used in this experiment.

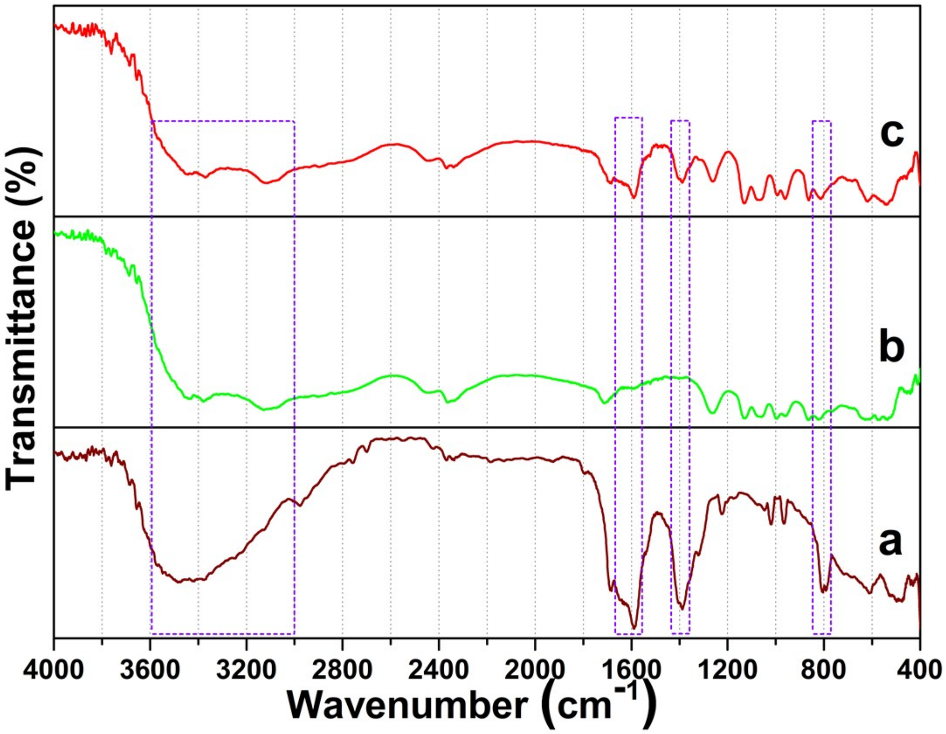

Fig. S35: IR spectra of (a) compound **1**, (b) HPO_4^{2-} and (c) compound **1** in presence of HPO_4^{2-}.

List of abbreviations used in the Table 2:

L_1 = 2-(4-carboxyphenyl)-1, 3-dioxoisoindoline-5-carboxylic acid; H_2btz = 1,5-bis(5-tetrazolo)-3-oxapentane; H_3ttz = 1,2,3-tris-[2-(5-tetrazolo)-ethoxy]propane; H_3BTB = 1,3,5-benzenetribenzoic acid; pdp = 2-(4,6-di(pyridine-2-yl)pyridine- 2-yl)pyridine; $C_{20}H_{10}N_2O_4S$ = 4,4′-(benzothiadiazole-4,7-diyl) dibenzoic acid; DEF = N, N'- diethyl formamide; DMF = N, N'- dimethyl formamide; H_2IPA = isophthalic acid; L_2 = 3- pyridylcarboxaldehyde nicotinoylhydrazone; TPOM = tetrakis(4-pyridyloxymethylene)methane; NH_2–BDC = 2-aminoterephthalic acid; H_3cpbda = 4,4′-((5-carboxy-1,3-phenylene)bis(oxy))dibenzoic acid; H_6L_3 = hexa[4-(carboxyphenyl)oxamethyl]-3-oxapentane acid; bipy = 2,2'-bipyridine ; bib = 4,4'- di(1 H-imidazol-1 -yl)-1,1'-biphenyl; tib = 1,3,5-tri(1 H-imidazol-1-yl)benzene; H_2ATA = 2-aminoterephthalic acid; L_4 = (E)-N′-(pyridin-4-ylmethylene)isonicotinohydrazide; H_2tza=1H-tetrazolate-5-acetic acid; H_3cpota = 2-(4-carboxyphenoxy)terephthalic acid; phen = 1,10-phenanthroline; TPPT = 1-{4-[4-(1H-1,2,4-triazol-1-yl)-phenoxy]phenyl}-1H-1,2,4-triazole; mtrb = 1,3-bis(1,2,4-triazole-4-ylmethyl)benzene; btc = 1,3,5-benzenetricarboxylate; H_6L_5 = (hexa[4-(carboxyphenyl)oxamethyl]-3-oxapentane acid); bbib = (1,4-bis(1 H-benzo[d]imidazol-1-yl)benzene); H_4tptc = p-terphenyl-2,2 ″,5 ″,5 ‴-tetracarboxylate acid; bib = 1,3-bis((imidazol-1-yl) benzene; bpanth =9,10-bis(4-pyridyl)anthracene; H_2oba =4,4 '-oxybis(benzoic acid); H_3ddpp = 2,5-di(2′,4′-dicarboxylpheny)pyridine acid; H_4mtb = 4-[tris(4-carboxyphenyl)methyl]benzoic acid; H_4L_6 = 5,5'-(1H-2,3,5-triazole-1,4-diyl)diisophthalic acid; H_2ipbpBr = cationic 1-(3,5-dicarboxyphenyl)-4,4`- bipyridinium bromide; H_2L^a = 2-(((2-hydroxy-3-methoxybenzyl)imino)methyl)-6-methoxyphenol; Piv = pivalic acid; HL_7 = 4′-(4-carboxyphenyl)−2,2′:6′,2″-terpyridine; HL_8 = 5-(triazol-1-yl)nicotinic acid; BTC = benzene-1,3,5-tricarboxylate; $H_3L^b\cdot BF_4$ = 2,4,6-tricarboxy-1-methylpyridinium tetrafluoroborate; btr = 4,4′-bis(1,2,4-triazole); H_3L_9 = p-terphenyl-3,4″,5-tricarboxylic acid; H_2L_{10} = 1,2-phenylenedioxydiacetic acid; H_3BTB = 1,3,5-benzenetribenzoate; H_3TZI = 5-(1H-tetrazol-5-yl)isophthalic acid; H_3BTB = 1,3,5-benzenetribenzoic acid and H_2BDC = 1,4-benzenedicarboxylic acid; H_3L_{11} = (4-carboxypiperidyl)-N-methylenephosphonic acid; TPA = 6-(1H-1,2,4-triazol-1-yl)pyridine-2-carboxylate; L_{12} = butanedioate; H_2L^c = 4-{bis(4-benzoic)amino}-4H-1,2,4-triazole; L^d = (6-[1-(4-carboxyphenyl)-1H-1,2,3-triazol-4-yl]nicotinic acid); H_2ppda = 4-(pyridin-3-yloxy)-phthalic acid and H_2npdc = naphthalene-1,4-dicarboxylic acid.